Unraveling different mechanisms of persulfate activation by graphite felt anode and cathode to destruct contaminants of emerging concern

Lingjun Bu[a,b,1], Jing Ding[c,1], Ningyuan Zhu[b,d], Minghao Kong[b], Yangtao Wu[a], Zhou Shi[a], Shiqing Zhou[a,*], Dionysios D. Dionysiou[b,*]

[a] *Key Laboratory of Building Safety and Energy Efficiency, Ministry of Education, Department of Water Engineering and Science, College of Civil Engineering, Hunan University, Changsha, 410082, China*
[b] *Environmental Engineering and Science Program, Department of Chemical and Environmental Engineering (ChEE), University of Cincinnati, Cincinnati, OH 45221-0012, USA*
[c] *State Key Laboratory of Urban Water Resources and Environment (SKLUWRE), School of Environment, Harbin Institute of Technology, Harbin, 150090, China*
[d] *State Key Laboratory of Soil and Sustainable Agriculture, Institute of Soil Sciences, Chinese Academy of Sciences, 71 East Beijing Road, Nanjing, 210008, China*

ARTICLE INFO

ABSTRACT

The electro-activation of persulfate (PS) by graphite felt (GF) electrode is a novel advanced oxidation process applied for the degradation of contaminants of emerging concern (CECs). Both GF anode and cathode can electro-activate PS to degrade CECs, including atrazine (ATZ), bisphenol S, ethinylestradiol, and ibuprofen. The study examines the removal performance of ATZ in sulfate, nitrate, and perchlorate electrolyte. The degradation of ATZ followed the order of sulfate $(36.3 \, L \, (Ah)^{-1}) > $ perchlorate $(22.2 \, L \, (Ah)^{-1}) > $ nitrate $(5.8 \, L \, (Ah)^{-1})$ in GF anode/PS system, while electrolytes had little influence on the degradation of ATZ $(15.8–21.3 \, L \, (Ah)^{-1})$ in GF cathode/PS system. The mechanisms of PS electro-activation by GF anode and GF cathode were compared and investigated for the first time, through kinetic experiments, radical identification, and products analysis. Quenching experiments demonstrated that $O_2^{\cdot-}$ and $^1O_2$ were generated in GF cathode/PS and GF anode/PS systems respectively, besides $HO^{\cdot}$ and $SO_4^{\cdot-}$. Degradation pathways of ATZ in these two systems showed slight difference, and a total of eight transformation products of ATZ were identified. Acute toxicity of the treated ATZ solution decreased at the beginning and then increased in both systems at electric charge of $0.11 \, Ah \, L^{-1}$. Furthermore, both GF electrodes/PS systems exhibited satisfactory performance for actual effluent from wastewater treatment plants in the presence of 30 mM perchlorate (with ATZ removal of 78% at electric charge of $0.11 \, Ah \, L^{-1}$), leaving a potential possibility for its practical application.

1. Introduction

With the frequent detections of contaminants of emerging concern (CECs) in surface water and groundwater, research studying on advanced oxidation processes (AOPs) have been in great demand to makeup the limitation of conventional treatments in wastewater treatment plants. As a vital branch of AOPs, electrochemical advanced oxidation process (EAOP) has attracted enhanced attention for the remediation of contaminated water [1–6]. Compared with other AOPs such as UV, sonochemical, and thermal based processes, EAOP could improve the utilization efficiency of energy appreciably by utilizing electrical energy directly. Researchers' attention mostly focused on anodic reactions in EAOP because oxidation reactions occurred on the anode, which can be used for the degradation of CECs [6–8]. Direct oxidation and electro-

generation of oxidants from water or electrolytes on the anode are responsible for such decontamination processes [9–11]. As oxygen evolution reactions on the anode can compete with the aforementioned reactions, oxygen evolution potential of anode is a very significant factor in EAOP. Therefore, the performance of EAOP strongly depends on the characteristics of electrode materials [12]. Many researchers have dedicated significant efforts to explore different materials for anodes to improve the degradation efficiency of contaminants in EAOP, including boron-doped diamond (BDD) [9,10,13], mixed metal oxide [14,15], Ti/Pt [12], and carbon-based electrodes [16]. Different oxidants (e.g. persulfate, ozone, ferrate, chlorine, and peroxides [9,17,18]) are proposed and confirmed to be generated on the anodes, but the corresponding reaction rates are rather slow. For example, persulfate (PS) would be generated and further activated in the sulfate electrolyte

[9,10], while the overall efficiency is limited by PS generation rate. This indicated the possibility of adding PS in EAOP. Implementation of PS in EAOP with BDD [19,20] and Ti/Pt [21] anodes has been investigated comprehensively in other studies and demonstrated enhanced degradation efficiency of pollutants, but the high cost of these anodes become a bottleneck for the wide application of EAOP.

The appearance of carbon-based electrodes gives researchers a promising alternative in EAOP because of their low cost, stable recyclability, and excellent conductivity [22,23]. These electrodes have been widely employed in capacitive deionization due to their large surface area [24–26]. Apart from this, carbon materials have been proven to exhibit satisfactory effect on activation of PS [27–29], without any metal ions leaching concerns. Furthermore, the employment of electric field on carbon materials can appreciably enhance the activation of PS and prolong the lifespan of carbon materials [30]. Song et al. reported degradation of sulfamethoxazole by electrochemical activation of PS using four kinds of carbon anodes (that is multi-walled carbon nanotube, graphite, black carbon, and granular activated carbon), and found PS was activated via both radical and nonradical mechanisms [31]. In contrast, Liu et al. investigated electro-activated PS by carbon fiber cathode and their results showed radical mechanism occurred on the cathode and generation of sulfate radical ($SO_4^{\cdot-}$) and hydroxyl radical ($HO^{\cdot}$) was confirmed [30]. Of note, most cathodes cannot efficiently activate PS because hydrogen evolution reactions are main reactions on the cathode, which means only hydrogen ions can accept electrons on cathodes. However, on graphite (carbon) felt (GF) cathode, other components (such as oxygen or PS) can accept electrons to be transformed to reactive species due to the high hydrogen evolution potential of GF electrode [32–34], which is always used in electro-Fenton processes, but disregarded in EAOPs. Until now, the differences between activation mechanisms of PS on GF anode and cathode have not been adequately explored and no study was dedicated to their comparison. Therefore, there is great need to further explore the potential of these electrodes and their mechanism of action.

Degradation of commonly detected CECs in the environment such as atrazine (ATZ), bisphenol S (BPS), ethinylestradiol (EE2), and ibuprofen (IBP), which have stable structure and are not easily biodegradable [35–38], was investigated to evaluate the performance of GF anode and cathode to electro-activate PS. As the reaction mechanisms of $HO^{\cdot}$ and $SO_4^{\cdot-}$ with ATZ have been elucidated in detail [39–41], determination of transformation products of ATZ and their evolution profiles can provide us new insights into the different mechanisms occurring on anode and cathode. Hence, ATZ was selected as target contaminant in the study of exploring the mechanism on the two types of electrodes.

Overall, the major objective of this study was to distinguish different mechanisms occurring on GF anode and cathode separately, using kinetic experiments, quenching experiments, and evolution profiles of transformation products of ATZ. Moreover, the performance and recyclability of GF electrode in synthetic and actual wastewater, variation of eco-toxicity and the transformation products during ATZ removal were also investigated in this study.

2. Materials and methods

2.1. Chemicals

ATZ, BPS, EE2, IBP, sodium perchlorate, sodium sulfate, sodium nitrate, sodium persulfate, ascorbic acid, methanol (MeOH), tert-butanol (TBA), superoxide dismutase (SOD), furfuryl alcohol (FFA), DMPO, and TEMPO were purchased from Sigma-Aldrich. GF electrode was obtained from Beijing Jixing, and stainless steel (SS) electrode was supplied from Hengshui steel. The actual wastewater samples were collected from biological treated effluent in a wastewater treatment plant.

2.2. Electrochemical degradation experiments

Undivided electrochemical configuration was made of a borosilicate glass reactor, with two electrodes (GF and SS) at a distance of 2.5 cm. The efficient working area of electrode was 6.25 cm^2. Treated solution was well-distributed with a magnetic bar stirring. All batch experiments were performed at a constant current density controlled by a DC power. Thirty mM NaClO$_4$ was applied to the system as supporting electrolyte to maintain the required conductivity. Target contaminant (ATZ, BPS, EE2, or IBP) of 2 μM and PS of 1.0 mM were added to the reaction solution before experiments. Quenching experiments were conducted with excess of scavengers (including TBA, MeOH, SOD, and FFA) to determine the responsible reactive species in the system. At each predetermined time interval, 0.9 mL solution was sampled and quenched immediately with 0.1 mL solution with 0.5 M ascorbic acid.

For N$_2$ purged experiments, N$_2$ was purged 30 min in advance to the ultrapure water to dilute solutions, and kept purging during the whole experiment to exclude all O$_2$ in the system. All the experiments were conducted at room temperature (25 ± 1 °C), and replicated three times.

Brand-new GF anode and cathode were used to perform the aforementioned experiments. Meanwhile, control experiment was conducted when GF anode and cathode were used for the 1st, 20th, 50th, and 100th times to examine their reuse performance.

Besides, the degradation of contaminants was described as a function of electric charge (Q, Ah L^{-1}).

2.3. Analytical methods

The concentration of ATZ, BPS, EE2, and IBP in solutions was measured using an HPLC (1200, Agilent, USA). Transformation products of ATZ were identified using a positive ESI HPLC (1290) tandem quadruple time-of-flight mass spectrometry (QTOF) (G6540 A, Agilent). Detailed conditions are described in SI Text S1. EPR tests were performed on a Bruker spectrometer (A300, German), with DMPO and TEMPO as the spin-trapping agent for radicals and $^1O_2$, respectively (details in SI Text S1). The concentrations of total organic carbon (TOC) were determined using a TOC analyzer (Shimadzu, Japan).

To figure out the variation of toxicity of ATZ before and after degradation, ECOSAR was employed to theoretically estimate the acute and chronic toxicity of ATZ and its products [42]. The acute toxicity of ATZ and its products was experimentally assessed using bacterial luminescence *Vibrio fischeri* (strain NRRL-B-11177). The details of analytical method were shown in SI Text S2.

3. Results and discussion

3.1. Nonselective degradation of CECs by activation of PS on the GF anode and cathode

Removal of ATZ in different systems was investigated and the results are presented in SI Fig. S1. Control experiment showed that removal of ATZ by GF adsorption and PS oxidation was negligible (less than 10% at time of 20 min). Combination of PS and GF (without electrolysis) slightly improved the degradation of ATZ because of the activation of PS by GF [31,43]. The implementation of electric field on GF electrodes (electrolysis) can also enhance the degradation of ATZ probably due to electro-adsorption or direct oxidation on the anode. Of note, more than 90% of ATZ was degraded in 10 min when PS was added to the electrolysis cell with GF electrodes. It was reported that carbon-based electrodes may activate PS at both anode and cathode [30,31]. Therefore, to confirm the statement and figure out the respective contribution of GF anode and GF cathode to the degradation of ATZ, SS electrode was selected as a counter electrode, which can hardly react with PS and contaminants.

As shown in Fig. 1a, comparable degradation of ATZ was achieved
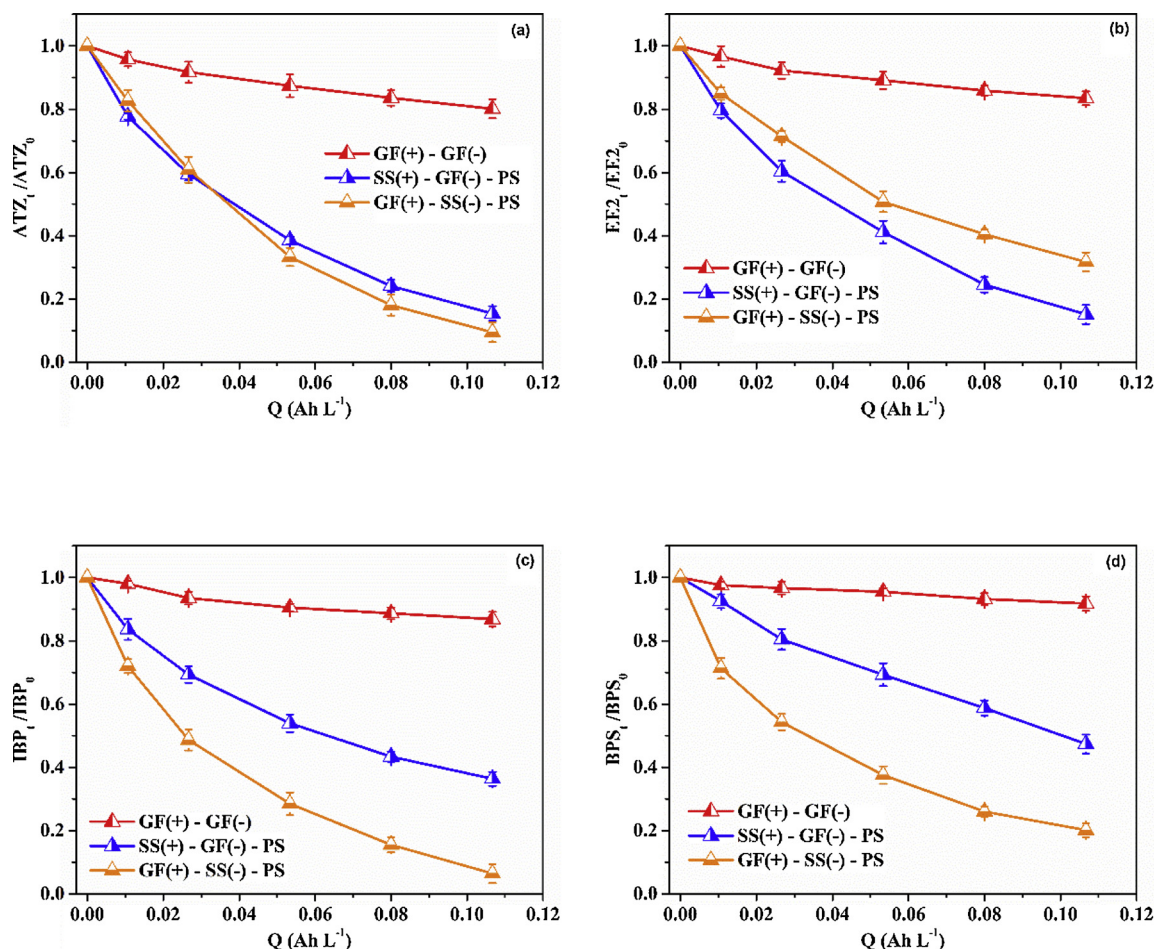
Fig. 1. Degradation of (a) ATZ, (b) EE2, (c) IBP, (d) BPS by GF anode/PS and GF cathode/PS systems. Experimental conditions: $[CECs]_0 = 2\,\mu M$, $[PS]_0 = 1.0\,mM$, $[NaClO_4]_0 = 30\,mM$, $pH_0 = 7.0$, current density $= 5.0\,mA\,cm^{-2}$. GF(+) – GF (-) means direct electrolysis using GF anode and GF cathode.

when GF was respectively used as anode and cathode, with removal of 90.6% and 84.6% at an electric charge of $0.10\,Ah\,L^{-1}$. EE2, IBP, and BPS can also be degraded efficiently by anodic and cathodic activation of PS (Fig. 1b–d). Notably, GF cathodic activation of PS performed better on degradation of EE2 (84.8%), while GF anodic activation of PS showed better performance on degradation of IBP (93.6%) and BPS (79.9%). Taking the difference of chemical structures of aforementioned CECs into consideration (SI Fig.S2), the results indicated that the corresponding mechanisms of activation of PS on GF anode and GF cathode are hypothesized to be different. Hence, the respective mechanism of PS activation on GF anode and cathode was investigated comprehensively from several different aspects in the following sections.

3.2. Effect of electrolyte and PS concentration on the performance of GF anode and cathode

Electrolyte is a key influence factor in EAOP to increase the ion conductivity of solutions. To satisfy the required conductivity, perchlorate, sulfate, and nitrate electrolytes have been routinely employed because of their inert character. As illustrated in Fig. 2, when GF was used as anode, the pseudo-first rate constants of degradation of ATZ followed the order of sulfate ($36.3\,L\,(Ah)^{-1}$) > perchlorate ($22.2\,L\,(Ah)^{-1}$) > nitrate ($5.8\,L\,(Ah)^{-1}$), which is consistent with the results of Farhat et al. [10] obtained from electrochemically activated sulfate by BDD anode. Similarly, the presence of sulfate promoted the generation of PS on GF anode, thereby leading to a drastic increase in rate constant of degradation of ATZ. However, the presence of nitrate
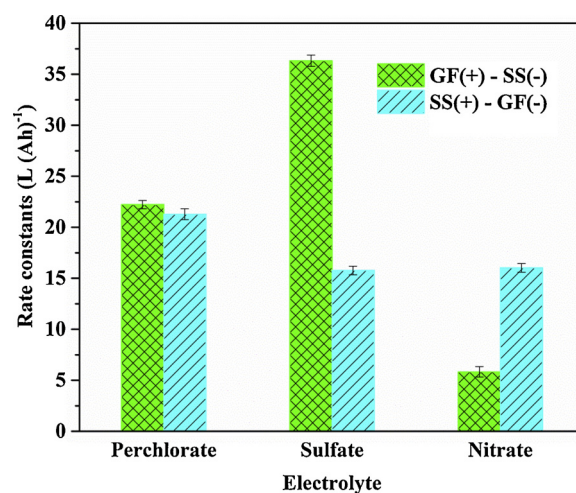
Fig. 2. The rate constants of degradation of ATZ in perchlorate, sulfate, and nitrate electrolytes by GF anode/PS and GF cathode/PS systems. Experimental conditions: $[ATZ]_0 = 2\,\mu M$, $[PS]_0 = 1.0\,mM$, $[NaClO_4]_0 = [Na_2SO_4]_0 = [NaNO_3]_0 = 30\,mM$, $pH_0 = 7.0$, current density $= 5.0\,mA\,cm^{-2}$.

inhibited ATZ degradation in GF anode/PS system because of the inert character of nitrate. On the other hand, electrolytes have no obvious effect on the degradation of ATZ when GF was applied as cathode. The corresponding rate constants ranged from $15.8–21.3\,L\,(Ah)^{-1}$ in these three electrolytes, suggesting that there is no reaction or interaction

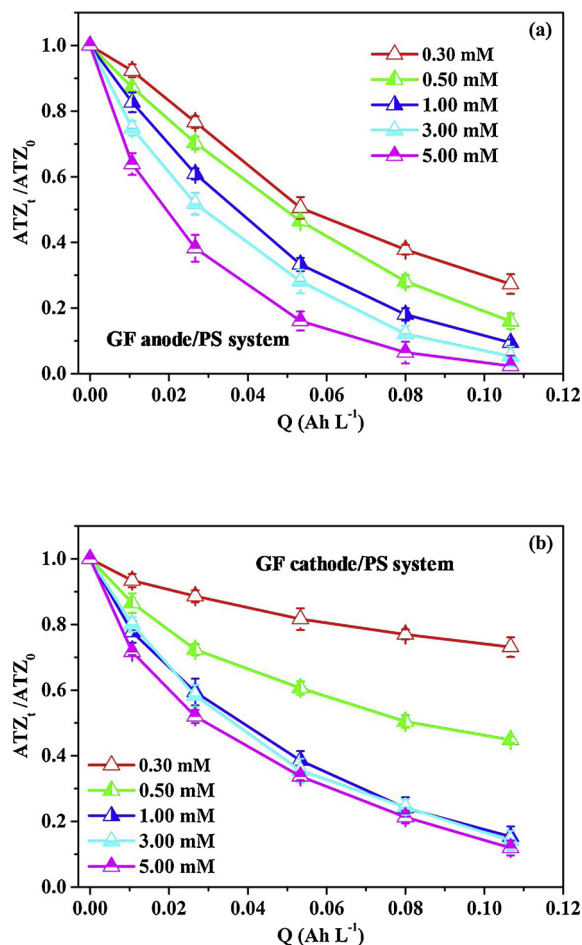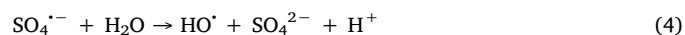$$Q(M) = \frac{I(A) \times T(s)}{96320 \times V(L)} \tag{1}$$

During the process, PS is usually considered as the electron acceptor on the cathode. However, because of electrostatic repulsive force, PS ions ($S_2O_8{}^{2-}$) can hardly approach GF cathode to accept electrons to be activated. Therefore, dissolved oxygen (DO) could be an important intermediate to get electrons to be transformed to superoxide radical anion ($O_2{}^{\bullet-}$), which then activate PS as shown in Eqs. (2)–(4) [44–46].

$$O_2 + e^- \rightarrow O_2{}^{\bullet-} \tag{2}$$

$$O_2{}^{\bullet-} + S_2O_8{}^{2-} \rightarrow O_2 + SO_4{}^{\bullet-} + SO_4{}^{2-} \tag{3}$$

$$SO_4{}^{\bullet-} + H_2O \rightarrow HO^{\bullet} + SO_4{}^{2-} + H^+ \tag{4}$$

To verify the proposed assumption, the effect of current density on the performance of GF cathode/PS system was investigated, and degradation of ATZ was promoted along with current density (1.0–10.0 mA cm^{-2}) (SI Fig. S3). The enhancement by the current density further confirmed the importance of electrons.

3.3. Identification of reactive species in GF cathode/PS and GF anode/PS systems

To examine the reactive species in GF cathode/PS and GF anode/PS systems, quenching experiments were conducted. The results of quenching experiment in GF anode/PS system are illustrated in Figs. 4a and S4a. As shown, the degradation rate constants of ATZ were almost the same when 50 mM TBA (7.1 L (Ah)$^{-1}$) and MeOH (6.7 L (Ah)$^{-1}$) were added in GF anode/PS system, indicating that HO$^{\bullet}$ existed in this system while SO$_4{}^{\bullet-}$ was not generated. Furthermore, when the dose of TBA and MeOH increased to 100 mM, the corresponding rate constants did not further decrease, suggesting the presence of another reactive species apart from HO$^{\bullet}$, which should be attributed to the activation of PS. Therefore, similar to the findings of Song and his colleagues [31], both radical and non-radical mechanisms occurred in GF anode/PS system. As reported by previous studies [27,47], carbon-based materials can activate PS or PMS to yield singlet oxygen ($^1O_2$), so the implementation of electric field is considered to enhance the generation of $^1O_2$. $^1O_2$ can hardly react with saturated alcohols such as MeOH and TBA, but reacts dramatically with electron-rich compounds (FFA) [48]. Hence, FFA was used to quench $^1O_2$ in GF anode/PS system with a rate constant of 1.2×10^8 M^{-1} s^{-1} [49]. Of note, FFA is also reported as an efficient quencher for radicals (SI Table S1) [50]. As shown in Fig. 4a, degradation of ATZ was further inhibited in the presence of excess FFA, confirming the generation of $^1O_2$ in GF anode/PS system. Then, EPR experiments were conducted in GF anode/PS system with DMPO and TEMPO and the corresponding spectra are shown in SI Fig. S5. The typical quartet spectrum of DMPO−HO$^{\bullet}$ (1: 2: 2: 1) was observed as marked in SI Fig. S5a, and a typical triplet spectrum with equal intensity (1: 1: 1) was also clearly observed in SI Fig. S5b. The results of EPR experiments further verified the existence of HO$^{\bullet}$ and $^1O_2$.

Different from that in GF anode/PS system, when 50 mM TBA and MeOH were respectively added to GF cathode/PS system, the degradation rate constant of ATZ decreased from 17.2 to 5.0 and 2.8 L (Ah)$^{-1}$ as shown in Figs. 4b and S4b. The results can indirectly confirm the presence of SO$_4{}^{\bullet-}$ and HO$^{\bullet}$ because TBA has a predominant role of quenching SO$_4{}^{\bullet-}$ and MeOH can quench both radicals (the second-order rate constants for the scavengers with radicals are shown in SI Table. S1) [51,52]. To confirm the assumption in previous section that $O_2{}^{\bullet-}$ was generated in GF cathode/PS system, SOD was used to quench $O_2{}^{\bullet-}$ in solution [53,54], and the corresponding rate constant decreased to 3.5 L (Ah)$^{-1}$ (Fig. 4b). Then, N$_2$ was purged to GF cathode/PS system to evaluate the effect of O$_2$ on ATZ degradation efficiency. Comparable degradation kinetics of ATZ were achieved in GF cathode/PS system when SOD was used as quencher (3.5 L (Ah)$^{-1}$) and N$_2$ purged (4.1 L (Ah)$^{-1}$), both indicating that $O_2{}^{\bullet-}$ is an important
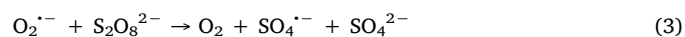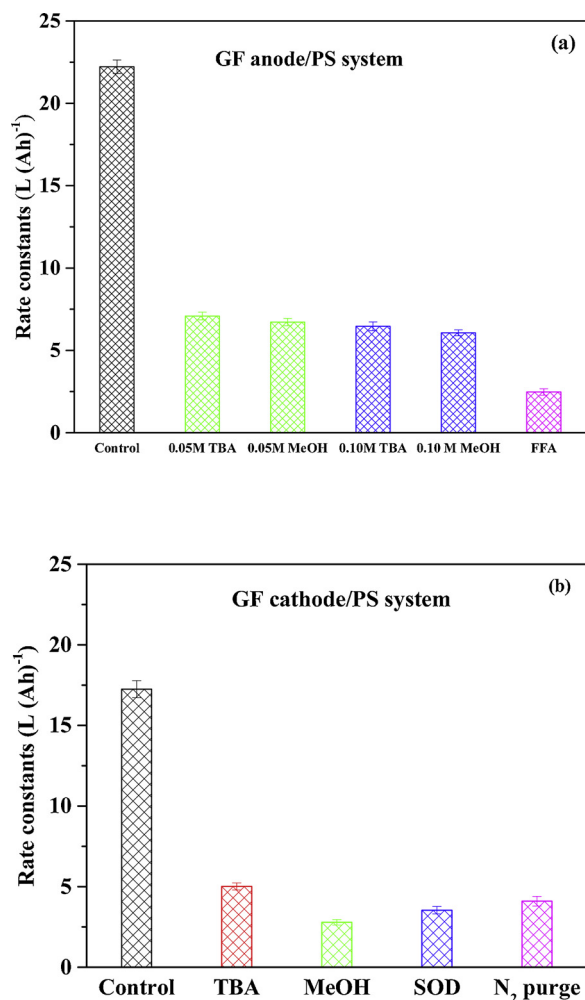
Fig. 3. Effect of PS dosage on the degradation of ATZ by (a) GF anode/PS and (b) GF cathode/PS systems. Experimental conditions: [ATZ]$_0$ = 2 μM, [PS]$_0$ = 0.3 ~ 5.0 mM, [NaClO$_4$]$_0$ = 30 mM, pH$_0$ = 7.0, current density = 5.0 mA cm^{-2}.

between electrolyte and GF cathode. Overall, the electrolyte plays an important role in the electro-activation of PS when GF was used as anode, but not as cathode.

Furthermore, the effect of PS concentration on degradation of ATZ by GF anodic and cathodic activation of PS was evaluated, and results are depicted in Fig. 3. As shown, the removal of ATZ by GF-anodic activated PS was appreciably enhanced when the concentration of PS increased from 0.3 mM to 5.0 mM, with the corresponding rate constant increasing from 12.5–33.7 L (Ah)$^{-1}$. The degradation rate constant of ATZ by GF-cathodic activated PS increased with PS concentration from 0.1 to 1.0 mM (from 2.8–17.2 L (Ah)$^{-1}$), in contrast, there is almost no further increase when the concentration of PS increased from 1.0–5.0 mM (from 17.2–19.0 L (Ah)$^{-1}$) (Fig. 3b). The phenomena demonstrated that GF anode could interact with PS and activate PS under the effect of electric field, while there were supposed to be some other factors influencing the activation of PS besides the concentration of PS on GF cathode. Since electrons move to cathode in electrochemical processes and GF cathode has a high hydrogen evolution potential, it is proposed that generated electrons on the cathode may play an important role in GF cathode/PS system. The concentration of electron in GF cathode/PS system was calculated to be 3.98 mM according to Eq. (1), which became speed-limiting factor when the concentration of PS increased to more than 3.98 mM. Therefore, the speed-limiting procedure of the GF cathode/PS system turned from mass transfer to electro control when the concentration kept increasing.

Fig. 4. Effect of different quenchers on the rate constants of degradation of ATZ by (a) GF anode/PS system and (b) GF cathode/PS system. Experimental conditions: $[ATZ]_0 = 2\,\mu M$, $[PS]_0 = 1.0\,mM$, $[NaClO_4]_0 = 30\,mM$, $[SOD] = 40,000\,U\,L^{-1}$, $[FFA] = 50\,mM$, $pH_0 = 7.0$, current density = 5.0 mA cm^{-2}.

intermediate to activate PS to yield $SO_4^{\cdot-}$ and $HO^{\cdot}$. Furthermore, a triplet EPR spectrum was observed in GF cathode/PS system (Fig. S5c), which is not a typical spectrum for radicals. However, as documented in previous research [55,56], the 1: 2: 1 triplet spectrum can be attributed to the oxidation of DMPOX by excess amount of radicals. The strong signal shown in SI Fig. S5c may overlap with the signal of the $O_2^{\cdot-}$, so the spectra of DMPO-$O_2^{\cdot-}$ adducts were not observed from the spectrum.

3.4. Proposed mechanism

As discussed above, the activation mechanisms of PS in GF anode/PS and GF cathode/PS systems are different. Specifically, in GF cathode/PS system (left part in Fig. 5), electron transfer is the dominant mechanism to activate PS because electrons move to cathode in electrochemical systems. However, due to the electrostatic repulsion between PS ($S_2O_8^{2-}$) and the surface of cathode, PS cannot approach the cathode surface to capture electrons. Therefore, oxygen (including DO and the generated oxygen from SS anode) was the most possible component that can act as electron captor in this system, which would be transformed to $O_2^{\cdot-}$ via electron transfer. As known, $SO_4^{\cdot-}$ is produced by reduction of PS with various one-electron reductants [52], and $O_2^{\cdot-}$ is a kind of peroxyl radicals with mild reducing property [46]. Consequently, $SO_4^{\cdot-}$ and $HO^{\cdot}$ are major species contributed to the

degradation of ATZ in GF cathode/PS system, and $O_2^{\cdot-}$ is the key intermediate.

On the other hand (GF anode/PS system), $S_2O_8^{2-}$ anions can move to the anode and some of them can be adsorbed on the electrode due to electrostatic attraction. $^1O_2$ can be generated when carbon materials interact with PS [27,47], so the employment of electric field may significantly enhance the corresponding reactions to produce more $^1O_2$. Besides, $HO^{\cdot}$ was generated from water molecule probably from two ways: (1) similar to reactions in BDD anode electrolysis system, GF adsorbed $HO^{\cdot}$ can be produced when electric field was implemented. (2) the excited PS molecule on GF anode can also transfer water to $HO^{\cdot}$ [31]. Therefore, both $HO^{\cdot}$ and nonradical ($^1O_2$) species can be generated in GF anode/PS system.

3.5. Comparison of transformation products of ATZ

The transformation products of ATZ in GF anode/PS and GF cathode/PS systems were identified using LC/QTOF-MS based on the corresponding value of mass-to-charge (m/z) and MS/MS patterns shown in SI Fig. S6. Because of the participation of $SO_4^{\cdot-}$, $HO^{\cdot}$, $^1O_2$, and the direct oxidation on anode, various reactions including electron transfer, dichlorination-hydroxylation etc, took place in these systems. The possible transformation products were summarized and presented in SI Table S2 and Fig. 6. As shown, two lateral chains and the chloride atom (marked in red) are the most susceptible sites of ATZ molecule, and four main schemes (SI Scheme S1– S4) can describe reactions occurred in these two systems. Specifically, electron transfer resulting from $SO_4^{\cdot-}$ can transform ATZ to a radical cation, which is in equilibrium with a nitrogen-centered radical. Nitrogen-centered radicals cannot react with oxygen, but they can transform to carbon-centered radicals via water catalyzed 1, 2-H shift, which can further transform to peroxyl radical via reaction with dissolved oxygen (k = 3×10^9 M^{-1} s^{-1} [57]) in solution (SI Scheme S1 [36]). Subsequent yield of olefination products (P1 and P7) can take place with the loss of per-hydroxyl radical ($HO_2^{\cdot}$). Similar transformation from ATZ to its carbonylation products (P2 and P8) can take place as shown in SI Scheme S2, of which $HO^{\cdot}$ attacked hydrogen at the α-position of the alkyl group to generate carbon centered radical [36,57]. Moreover, dealkylation is the predominant reaction occurred in these two systems, which is based on Chugaev reaction (SI Scheme S3) [19]. Both lateral chains in ATZ molecule can be oxidized to amine. Notably, the carbon-centered radical on N-isopropyl group has a higher energy than that on *N*-ethyl group [39], resulting in the prevalence of transformation product with *N*-isopropyl group (P3) (Fig. 7). Dechlorination - hydroxylation is another commonly-occurred reaction during the degradation of ATZ (SI Scheme S4): An organic radical cation can be generated at first by electron transfer via reaction between ATZ and $SO_4^{\cdot-}$. Then, HO from water molecular can undergo nucleophilic substitution reaction to replace the chloride atom on the radical anion, because water is a typical nucleophilic reagent. Besides, ipso attack by $HO^{\cdot}$ may also occur at the position of chloride atom to lead to the elimination of Cl [58].

Moreover, the evolution profiles of each product in GF anode/PS and GF cathode/PS systems were determined to further evaluate (Fig. 7) the differences between the two systems. Among the eight products, P1 was not detected in GF cathode/PS system, and P6 was not detected in GF anode/PS system. Apart from P1 and P6, P2 and P3 exhibited similar concentrations in these two systems (Fig. 7b and c). Similar trend for evolution profiles of P5 was observed (Fig. 7e), while the corresponding concentration in GF anode/PS system was much higher than that in GF cathode/PS system. For P4, P7, and P8, totally different evolution profiles were observed in these two systems (Fig. 7d–h). The aforementioned phenomenon indicated that ATZ experienced different pathways when GF was used as anode and cathode to activate PS, which should be attributed to the respective involvement of $O_2^{\cdot-}$ and $^1O_2$. On the other hand, six transformation products reached their maximum concentration and showed decreasing trends
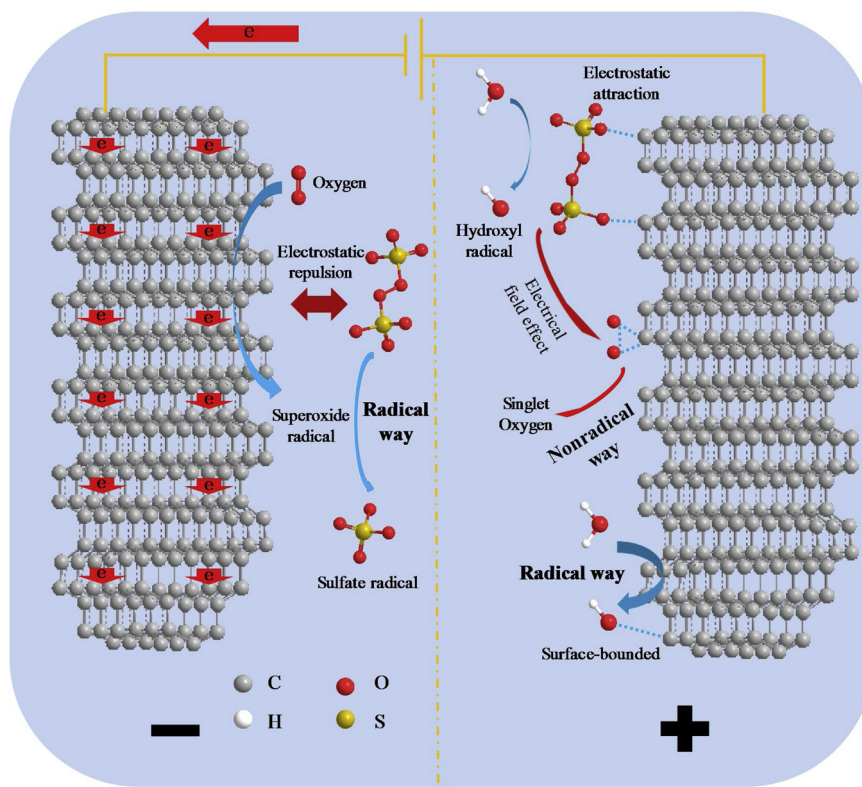
Fig. 5. Proposed mechanism of PS activation on GF anode and GF cathode.

during the degradation of ATZ in GF anode/PS system, while up to four products kept increasing in GF cathode/PS system. Furthermore, when ATZ solution was treated with GF anode/PS system, the corresponding TOC decreased by 19%, while 12% TOC was removed by GF cathode/PS system (SI Fig. S7), revealing that degradation of ATZ was more complete in GF anode/PS system than that in GF cathode/PS system.

Notably, the increasing concentrations of four products in GF cathode/PS system left a potential possibility of increasing cytotoxicity in solutions. To figure out the issue, acute and chronic toxicity of ATZ and its transformation products were calculated using ECOSAR. All
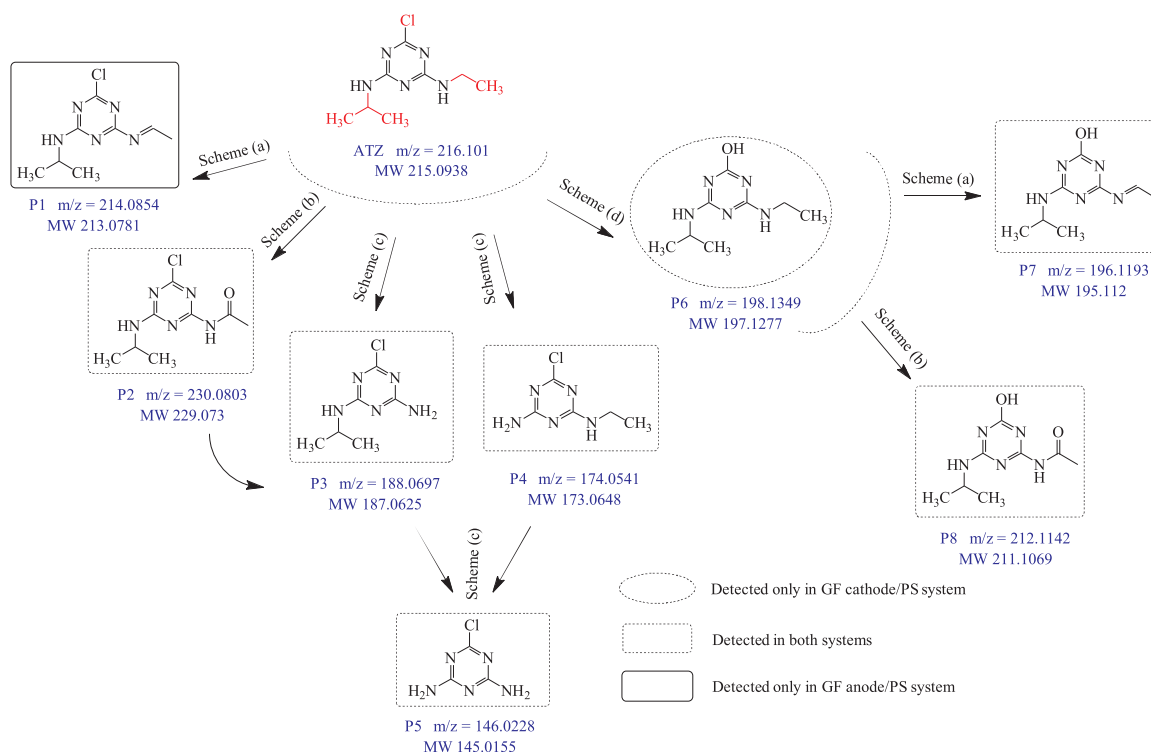

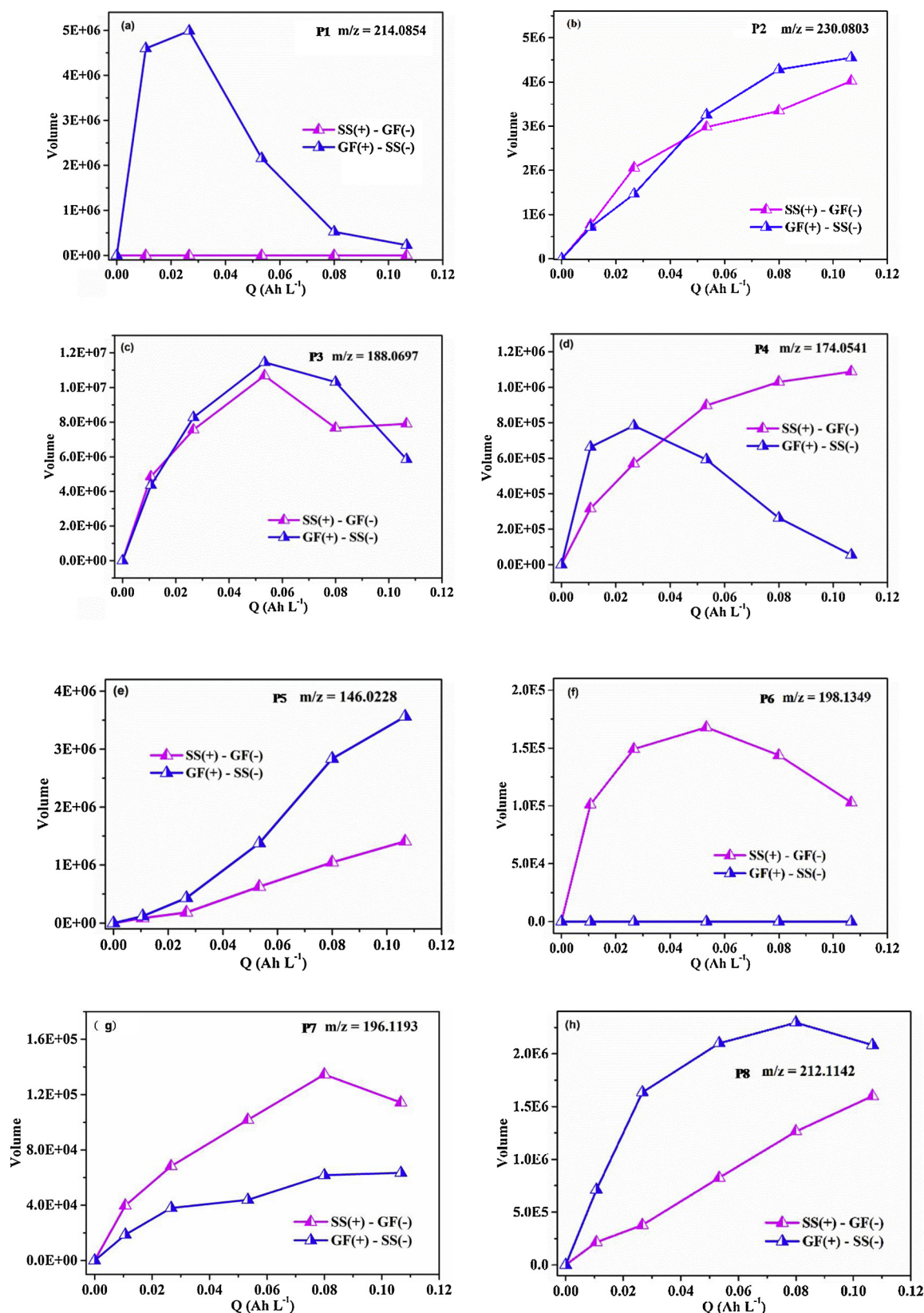**Fig. 6.** Proposed degradation pathway of ATZ by GF electrode/PS system.

Fig. 7. Evolution profiles of transformation products of ATZ in GF anode/PS and GF cathode/PS systems. Experimental conditions: $[ATZ]_0 = 2\,\mu M$, $[PS]_0 = 1.0\,mM$, $[NaClO_4]_0 = 30\,mM$, $pH_0 = 7.0$, current density = $5.0\,mA\,cm^{-2}$.

detected products showed lower toxicity than the parent compound as depicted in SI Table S3. However, the calculated results cannot guarantee the decrease of the acute toxicity of the reaction solution, because

(1) some products with higher toxicity may not be detected in this study; and (2) ATZ and its products may show combined toxicity when they exist simultaneously. Therefore, *Vibrio fischeri* was used to
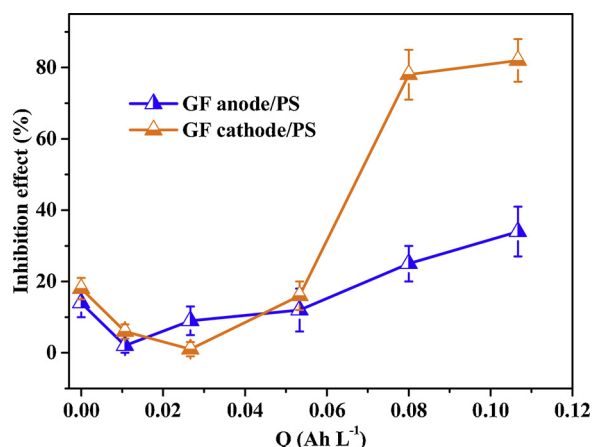
Fig. 8. Variation of acute toxicity of ATZ solution treated by GF anode/PS and GF cathode/PS systems. Experimental conditions: $[ATZ]_0 = 2\,\mu M$, $[PS]_0 = 1.0\,mM$, $[NaClO_4]_0 = 30\,mM$, $pH_0 = 7.0$, current density $= 5.0\,mA\,cm^{-2}$.

determine the variation of acute toxicity before and after reaction in GF anode/PS and GF cathode/PS systems, and results were presented in Fig. 8. The acute toxicity of both systems decreased at the beginning and then increased, indicating that some kinds of further oxidation products of ATZ (with higher toxicity) were accumulated in the systems. The aforementioned observation also suggested that results of ECOSAR are not necessarily reliable when variation of acute toxicity is evaluated.

3.6. Application potential of GF anode/PS and GF cathode/PS systems

To evaluate the potential of GF-based/PS systems in practical application, the biological effluent from wastewater treatment plant (WWTP) was used as the background to test the degradation of ATZ (water quality parameters of the effluent were presented in SI Table S4). As shown in SI Fig. S8, when effluent from WWTP was spiked with ATZ, the degradation of ATZ in both systems was significantly inhibited because of the lack of supporting electrolytes and presence of various water components (natural organic matters (denoted as COD) and alkalinity). Even so, when the effluent was used as the background with the presence of 30 mM perchlorate, the degradation of ATZ was only inhibited slightly compared to that in DI water, which should be attributed to the presence of chloride. Chloride ions in effluent can be transformed to active chlorine on the anode [59], which can accelerate the degradation of CECs. The aforementioned results indicated that GF-based/PS systems are efficient to remove CECs in actual waters with enough electrolytes.

Furthermore, the recyclability of GF electrodes in aforementioned systems was also investigated. As mentioned in previous studies, the recycle performance of carbon materials to activate PS was relatively poor [30], which limited their wide use in practical application. However, with the assistance of electric field, the reuse performance of GF was significantly enhanced as shown in SI Fig. S9. To better determine the reasons, the general morphologies of brand-new GF electrode, GF anode used after 100 times, and GF cathode used after 100 times were analyzed by SEM, and the corresponding images were presented in SI Fig. S10. The virgin GF electrode has a smooth surface as shown in Fig. S10a. When it was used as anode for 100 times, the surface was obviously destructed or polluted probably because of the interaction between GF anode and PS anions (Fig. S10b). However, the degradation of ATZ did not show obvious decrease after 100 times in GF anode/PS system, which indicated that smoothness of GF surface has few effects on the performance of GF anode/PS system. Besides, when GF cathode was used after 100 times, the morphology of GF cathode

was almost the same as that of the virgin GF electrode (Fig. S10c), but around 10% decline was observed after 100 times reuse in GF cathode/PS system, which may be attributed to the decrease of electron transfer efficiency due to long-time operation. Overall, the GF electrodes showed satisfying effect on recyclability to degrade ATZ.

4. Conclusions

The study provides a detailed investigation on the comparison of the PS electro-activation mechanisms on GF anode and GF cathode, and the following conclusions can be obtained:

(1) The removal efficiency of all investigated CECs (ATZ, BPS, EE2, and IBP) were more than 50% in GF anode/PS and GF cathode/PS systems at the electric charge of $0.10\,Ah\,L^{-1}$. GF anode/PS system performed better on degradation of ATZ, BPS, and IBP than GF cathode/PS system, while EE2 was degraded more easily in GF cathode/PS system.

(2) Electrolyte is a significant influence factor in GF anode/PS system, where ATZ was degraded following the order of sulfate > perchlorate > nitrate, but electrolyte had no obvious effect on the degradation of ATZ in GF cathode/PS system. Degradation of ATZ was enhanced with the concentration of PS in GF anode/PS system, whereas removal efficiency of ATZ was associated with the concentration of electrons in GF cathode/PS system.

(3) Quenching experiments showed that different reactive oxygen species ($^1O_2$ and $O_2^{\cdot-}$) played important roles for the degradation of ATZ in GF anode/PS and GF cathode/PS systems: $^1O_2$ and $OH^{\cdot}$ were generated because of the interaction between PS and GF anode, while $O_2^{\cdot-}$ was generated from dissolved oxygen by accepting electrons on GF cathode. Generated $O_2^{\cdot-}$ acted as the activator for PS in GF cathode/PS system.

(4) A total of eight transformation products of ATZ and their respective evolution profiles were determined, and acute toxicity decreased at the beginning and then increased in both systems. The degradation performance of ATZ was efficient in actual wastewater with enough electrolytes, and GF electrodes can be used to effectively remove ATZ after reuse for 100 times.

Acknowledgement

Appendix A. Supplementary data

Supplementary material related to this article can be found, in the online version, at doi:https://doi.org/10.1016/j.apcatb.2019.04.030.

References

[1] E. Brillas, C.A. Martínez-Huitle, Appl. Catal. B: Environ. 166 (2015) 603–643.
[2] L. Bu, S. Zhou, Z. Shi, C. Bi, S. Zhu, N. Gao, Sep. Purif. Technol. 178 (2017) 66–74.
[3] J. Ding, Q. Zhao, Y. Zhang, L. Wei, W. Li, K. Wang, Water Res. 74 (2015) 122–131.
[4] F.C. Moreira, R.A.R. Boaventura, E. Brillas, V.J.P. Vilar, Appl. Catal. B: Environ. 202 (2017) 217–261.
[5] J. Radjenovic, D.L. Sedlak, Environ. Sci. Technol. 49 (2015) 11292–11302.
[6] C.A. Martínez-Huitle, M.A. Rodrigo, I. Sirés, O. Scialdone, Chem. Rev. 115 (2015)

13362–13407.

[7] I. Sirés, E. Brillas, M.A. Oturan, M.A. Rodrigo, M. Panizza, Environ. Sci. Pollut. R. 21 (2014) 8336–8367.

[8] S. Zhou, L. Bu, Z. Shi, C. Bi, Q. Yi, Chem. Eng. J. 306 (2016) 719–725.

[9] L. Bu, S. Zhou, Z. Shi, L. Deng, N. Gao, Chemosphere 168 (2017) 1309–1316.

[10] A. Farhat, J. Keller, S. Tait, J. Radjenovic, Environ. Sci. Technol. 49 (2015) 14326–14333.

[11] A. Thiam, E. Brillas, J.A. Garrido, R.M. Rodríguez, I. Sirés, Appl. Catal. B: Environ. 180 (2016) 227–236.

[12] J. Jeong, C. Kim, J. Yoon, Water Res. 43 (2009) 895–901.

[13] L.W. Matzek, M.J. Tipton, A.T. Farmer, A.D. Steen, K.E. Carter, Environ. Sci. Technol. 52 (2018) 5875–5883.

[14] R. Xie, X. Meng, P. Sun, J. Niu, W. Jiang, L. Bottomley, D. Li, Y. Chen, J. Crittenden, Appl. Catal. B: Environ. 203 (2017) 515–525.

[15] S. Zhou, L. Bu, Y. Yu, X. Zou, Y. Zhang, Chemosphere 165 (2016) 381–387.

[16] G. Lissens, J. Pieters, M. Verhaege, L. Pinoy, W. Verstraete, Electrochim. Acta 48 (2003) 1655–1663.

[17] C.A. Martinez-Huitle, S. Ferro, Chem. Soc. Rev. 35 (2006) 1324–1340.

[18] M. Panizza, G. Cerisola, Chem. Rev. 109 (2009) 6541–6569.

[19] L. Bu, S. Zhu, S. Zhou, Chemosphere 195 (2018) 236–244.

[20] H. Song, L. Yan, J. Jiang, J. Ma, Z. Zhang, J. Zhang, P. Liu, T. Yang, Water Res. 128 (2018) 393–401.

[21] H. Song, L. Yan, J. Ma, J. Jiang, G. Cai, W. Zhang, Z. Zhang, J. Zhang, T. Yang, Water Res. 116 (2017) 182–193.

[22] C. Nie, Z. Ao, X. Duan, C. Wang, S. Wang, T. An, Chemosphere 206 (2018) 432–438.

[23] X. Li, S. Chen, X. Quan, Y. Zhang, Environ. Sci. Technol. 45 (2011) 8498–8505.

[24] H. Li, T. Lu, L. Pan, Y. Zhang, Z. Sun, J. Mater. Chem. 19 (2009) 6773–6779.

[25] G. Wang, B. Qian, Q. Dong, J. Yang, Z. Zhao, J. Qiu, Sep. Purif. Technol. 103 (2013) 216–221.

[26] L. Yang, Z. Shi, W. Yang, Electrochim. Acta 153 (2015) 76–82.

[27] X. Cheng, H. Guo, Y. Zhang, X. Wu, Y. Liu, Water Res. 113 (2017) 80–88.

[28] X. Duan, Z. Ao, L. Zhou, H. Sun, G. Wang, S. Wang, Appl. Catal. B: Environ. 188 (2016) 98–105.

[29] H. Lee, H.-J. Lee, J. Jeong, J. Lee, N.-B. Park, C. Lee, Chem. Eng. J. 266 (2015) 28–33.

[30] Z. Liu, C. Zhao, P. Wang, H. Zheng, Y. Sun, D.D. Dionysiou, Chem. Eng. J. 343 (2018) 28–36.

[31] H. Song, L. Yan, J. Jiang, J. Ma, S. Pang, X. Zhai, W. Zhang, D. Li, Chem. Eng. J. 344 (2018) 12–20.

[32] A. Dirany, I. Sirés, N. Oturan, A. Özcan, M.A. Oturan, Environ. Sci. Technol. 46 (2012) 4074–4082.

[33] C. Trellu, N. Oturan, F.K. Keita, C. Fourdrin, Y. Pechaud, M.A. Oturan, Environ. Sci. Technol. 52 (2018) 7450–7457.

[34] M.A. Oturan, J. Pinson, J. Phys. Chem. 99 (1995) 13948–13954.

[35] L. Bu, C. Bi, Z. Shi, S. Zhou, Chem. Eng. J. 321 (2017) 642–650.

[36] H.V. Lutze, S. Bircher, I. Rapp, N. Kerlin, R. Bakkour, M. Geisler, C. von Sonntag, T.C. Schmidt, Environ. Sci. Technol. 49 (2015) 1673–1680.

[37] G. Grill, J. Li, U. Khan, Y. Zhong, B. Lehner, J. Nicell, J. Ariwi, Water Res. 145 (2018) 707–720.

[38] Y. Gao, J. Jiang, Y. Zhou, S.-Y. Pang, J. Ma, C. Jiang, Y. Yang, Z.-s. Huang, J. Gu, Q. Guo, Water Res. 131 (2018) 208–217.

[39] Y. Huang, C. Han, Y. Liu, M.N. Nadagouda, L. Machala, K.E. O'Shea, V.K. Sharma, D.D. Dionysiou, Appl. Catal. B: Environ. 221 (2018) 380–392.

[40] J.A. Khan, X. He, N.S. Shah, H.M. Khan, E. Hapeshi, D. Fatta-Kassinos, D.D. Dionysiou, Chem. Eng. J. 252 (2014) 393–403.

[41] C. Luo, J. Jiang, C. Guan, J. Ma, S. Pang, Y. Song, Y. Yang, J. Zhang, D. Wu, Y. Guan, RSC Adv. 7 (2017) 29255–29262.

[42] L. Bu, S. Zhou, S. Zhu, Y. Wu, X. Duan, Z. Shi, D.D. Dionysiou, Water Res. 146 (2018) 288–297.

[43] X. Duan, H. Sun, J. Kang, Y. Wang, S. Indrawirawan, S. Wang, ACS Catal. 5 (2015) 4629–4636.

[44] G. Fang, C. Liu, J. Gao, D.D. Dionysiou, D. Zhou, Environ. Sci. Technol. 49 (2015) 5645–5653.

[45] G.-D. Fang, D.D. Dionysiou, S.R. Al-Abed, D.-M. Zhou, Appl. Catal. B: Environ. 129 (2013) 325–332.

[46] G. Mark, M.N. Schuchmann, H.-P. Schuchmann, C. von Sonntag, J. Photochem. Photobiol. A: Chem. 55 (1990) 157–168.

[47] X. Duan, H. Sun, Z. Shao, S. Wang, Appl. Catal. B: Environ. 224 (2017) 973–982.

[48] M.A.J. Rodgers, J. Am. Chem. Soc. 105 (1983) 6201–6205.

[49] Y. Zhou, J. Jiang, Y. Gao, J. Ma, S.-Y. Pang, J. Li, X.-T. Lu, L.-P. Yuan, Environ. Sci. Technol. 49 (2015) 12941–12950.

[50] C. Minero, G. Mariella, V. Maurino, D. Vione, E. Pelizzetti, Langmuir 16 (2000) 8964–8972.

[51] G.V. Buxton, C.L. Greenstock, W.P. Helman, A.B. Ross, J. Phys. Chem. Ref. Data 17 (1988) 513–886.

[52] P. Neta, R.E. Huie, A.B. Ross, J. Phys. Chem. Ref. Data 17 (1988) 1027–1284.

[53] Y. Chen, X. Zhang, S. Feng, Environ. Sci. Technol. 52 (15) (2018) 8283–8291.

[54] H. Jung, T.S. Chadha, D. Kim, P. Biswas, Y.-S. Jun, Chem. Commun. (Camb.) 53 (2017) 4445–4448.

[55] J.M. Fontmorin, R.C. Burgos Castillo, W.Z. Tang, M. Sillanpää, Water Res. 99 (2016) 24–32.

[56] K. Guo, J. Zhang, A. Li, R. Xie, Z. Liang, A. Wang, L. Ling, X. Li, C. Li, J. Fang, Environ. Sci. Technol. Let. (2018).

[57] A. Tauber, C. Von Sonntag, Acta Hydroch, Hydrob. 28 (2000) 15–23.

[58] B. Balci, N. Oturan, R. Cherrier, M.A. Oturan, Water Res. 43 (2009) 1924–1934.

[59] J.T. Jasper, O.S. Shafaat, M.R. Hoffmann, Environ. Sci. Technol. 50 (2016) 10198–10208.